Dalton Transactions

PAPER

View Article Online
View Journal | View Issue



Cite this: *Dalton Trans.*, 2018, **47**, 7541

# Mechanism of H adatoms improving the $O_2$ reduction reaction on the Zn-modified anatase $TiO_2$ (101) surface studied by first principles calculation†

Liangliang Liu,[a,c] Chongyang Li,[b,c] Man Jiang,[d] Xiaodong Li,[c] Xiaowei Huang,*[a] Zhu Wang*[c] and Yu Jia*[a]

Received 10th March 2018,
Accepted 2nd May 2018

DOI: 10.1039/c8dt00931g

rsc.li/dalton

First principles calculations were performed to cast insight into the mechanism of the improvement of $O_2$ reduction reaction (ORR) activity by Zn and H interstitials on the anatase $TiO_2$ (101) surface. For the Zn-modified anatase $TiO_2$ (101) surface, both surface and subsurface Zn interstitials could contribute to $O_2$ adsorption and dissociation, but the dissociation barriers of $O_2$ molecules are still too high, which limits the ORR activity. After a H adatom is introduced onto the Zn-modified anatase $TiO_2$ (101) surface, the highest energy barriers are greatly reduced compared with those of the Zn-modified surface. Meanwhile, it is observed that the dissociation barriers decrease almost linearly with the increase of the charge difference of adsorption $O_2$ between initial and transition state configurations. Specifically, subsurface Zn and surface H interstitials facilitate $O_2$ dissociation and subsequent oxidation reactions, and further frequency analysis shows that these dissociation processes are frequent even at the room temperature of 300 K. In a word, this work provides a theoretical support to design a high ORR activity catalyst of the $TiO_2$ nanocrystal comparable to precious Pt catalysts.

## 1. Introduction

$TiO_2$, in typical photocatalysis and as a heterogeneous catalyst, has attracted a lot of attention because it exhibits high activity for a variety of different reactions, such as hydrogen production, organic pollutant degradation, and CO oxidation.[1–5] Surface adsorbed $O_2$ molecules can be used as electron scavengers to enhance $TiO_2$ photocatalysis activity, and the oxygen reduction reaction (ORR) plays a critical role in the rate-limiting step in photocatalysis.[1,2,6] The catalytic activity for the ORR strongly depends on $O_2$ adsorption energy, dissociation energy barrier, and the binding energy of dissociation O adatoms.[7,8] A good ORR catalytic activity requires intermediate $O_2$ bonding to the active site, facilitating both O–O bond breaking and subsequent oxidation reactions of O adatoms. However, the slow reaction kinetics of oxygen reduction stems from $O_2$'s inability to adsorb onto the clean anatase $TiO_2$ (A-$TiO_2$) surface.[9,10] Previous research studies show that $O_2$ could not be adsorbed onto a clean A-$TiO_2$ surface, while the negatively charged surface and defects are reported to facilitate $O_2$ adsorption.[9–12] Therefore, the influence of $TiO_2$ surface modification on $O_2$ adsorption and dissociation is explored from the experimental and theoretical research studies, and these modifications include H adatoms, $TiO_2$ intrinsic defects, noble metal deposition and so on.[10–14]

The main intrinsic defects in $TiO_2$ are Ti interstitials and O vacancies,[15,16] and these two types of defects play a central role in the surface physicochemical properties of $TiO_2$; meanwhile, these defects are reported to contribute to the reduction of $O_2$ molecules.[11,12] Research by Setvin *et al.* shows that with the help of the surface $O_2$ molecule, a subsurface O vacancy could easily diffuse to the surface and react with the adsorbed $O_2$ molecule to form a bridging $(O_2)_O$ dimer, and the energy barrier is much lower than that of the O vacancy diffusion without the surface $O_2$ molecule.[11] In a recent study, we found that a subsurface Ti interstitial can enhance the ORR catalytic activity of the A-$TiO_2$ (101) surface by reaction with two adsorbed $O_2$ molecules.[17] Moreover, deposition of noble

[a]*Key Lab for Special Functional Materials of Ministry of Education, Collaborative Innovation Center of Nano Functional Materials and Applications, Henan Province, Henan University, Kaifeng 475004, PR China. E-mail: jiayu@zzu.edu.cn, xiaohuang_30@126.com; Tel: +86-037122357375*
[b]*College of Electric Power, North China University of Water Resources and Electric Power, Zhengzhou 450045, China*
[c]*School of Physics and Technology, Wuhan University, Wuhan 430072, PR China. E-mail: wangz@whu.edu.cn*
[d]*Key Laboratory of Neutronics and Radiation Safety, Institute of Nuclear Energy Safety Technology, Chinese Academy of Sciences, Hefei, Anhui, 230031 China*
†Electronic supplementary information (ESI) available. See DOI: 10.1039/c8dt00931g

metal, Au or Pt on the $TiO_2$ surface is identified to be another effective way to improve catalytic activity by modifying $O_2$ reduction.[10,14,18] However, for the above modified methods, the high formation energies of the O vacancy and Ti interstitial result in defect densities that are too low to significantly increase the rate of the ORR,[15,16] and noble metals are quite expensive, which is not beneficial for wide applications in industry. Therefore, it is critical to develop an effective and economical method to achieve $TiO_2$ catalysts with high ORR catalytic activity.

Inducing heterogeneous atoms, as the most straightforward way to modify $TiO_2$, has been widely used in order to promote $TiO_2$ catalytic activity, which is able to regulate the band structure of $TiO_2$ in order to extend the spectral response of $TiO_2$.[1,4] In fact, the dopants in $TiO_2$ could also increase the ORR of the $TiO_2$ surface.[19–22] For example, a theoretical study by Muhich *et al.* indicates that B and C interstitials significantly improve the $TiO_2$ photocatalytic reduction of $O_2$.[19] Nb-Doped $TiO_2$ is also identified to be an effective method to enhance the ORR, and thus to be an alternative support for PEM fuel cells.[20–22] Yet, to the best of our knowledge, although these research studies have paid attention to the effect of dopants on the reduction of $O_2$ molecules, the reaction process and the mechanism are not all clear, and how the dopants specifically, transition metals can promote the $O_2$ dissociation reaction is still an open question. Since metal Zn is one of the typical 3d transition metals and abundant on Earth, a lot of research studies focus on the effect of Zn doping on $TiO_2$ photocatalytic activity and show that Zn-doped $TiO_2$ could change the band structure of $TiO_2$ and increase the range of light absorption,[1,23,24] while no existing works attempt to examine the ORR activity from the Zn doping perspective.

When a Zn atom is induced into the $TiO_2$ surface, it may substitute Ti atoms or occupy the interstitial site in the $TiO_2$ surface.[1,3] For the case of a Zn substitution, a Zn atom occupies a Ti atom site and provides two electrons for the $TiO_2$ lattice, and thus it will give rise to p-type $TiO_2$.[23,24] However, p-type $TiO_2$ is not good for $O_2$ adsorption. In fact, the $O_2$ molecule does not adsorb onto stoichiometric and p-type $TiO_2$ surfaces, and excess electrons are required.[1,9,12] The excess electron transfer from the surface to the oxygen molecule is essential for oxygen adsorption. For the case of Zn interstitials, a Zn interstitial could provide two excess electrons to the $TiO_2$ surface and enhance $O_2$ adsorption, which may be good for the $O_2$ reduction reaction on the $TiO_2$ surface. Therefore, in this article, the density functional theory is used to calculate $O_2$ adsorption and dissociation to quantify the effect of Zn interstitials.

After a Zn atom is introduced on and near the A-$TiO_2$ (101) surface, both surface and subsurface Zn interstitials could contribute to $O_2$ adsorption and dissociation, but the dissociation barriers of the $O_2$ molecule are too high, which limits the ORR activity. Since H adatoms could facilitate $O_2$ dissociation based on previous studies,[13,25] in order to further reduce dissociation barriers, a H adatom is introduced on the Zn-modified A-$TiO_2$ (101) surface. The calculated results show that after a H atom is adsorbed onto the $TiO_2$ surface, at the transition state, more excess electrons could transfer to two O adatoms, and two adsorbed O adatoms form strong chemical bonds with surface Ti atoms and H atoms. Therefore, the energy barriers of $O_2$ dissociation are greatly reduced compared with those of the Zn-modified A-$TiO_2$ surface. In particular, with the synergistic effect of surface H and subsurface Zn interstitials, the adsorbed $O_2$ is easy to dissociate and participate in the subsequent oxygen reaction, and frequency analysis shows that the $O_2$ dissociation processes frequently happen even at the room temperature of 300 K.

## 2. Computational detail

First-principles calculations are used to study the $O_2$ adsorption and dissociation on an A-$TiO_2$ (101) surface, and the calculations are performed using the Vienna *Ab initio* Simulation Package (VASP).[26–28] In this article, the GGA-PBE exchange–correlation functional[29–31] coupled with projector augmented wave (PAW) pseudopotentials is applied in the calculations. The GGA + U method is used to calculate the charge distribution of the excess electrons induced by the Zn and H interstitial atoms, and the value of U for Ti 3d is 4.2 eV[32,33] while $O_2$ molecule adsorption and dissociation on the $TiO_2$ surface are calculated with the GGA-PBE method. In previous research, Du *et al.* show that energy barrier for $O_{ad}$ diffusion with GGA + U differs slightly from that with GGA, and the reaction path of $O_2$ using DFT + U agrees with that from DFT.[34] Meanwhile, some research studies show that the GGA functional could correctly describe the effect of the surface or subsurface defects on reaction processes of adsorbed $O_2$ molecules on the $TiO_2$ surface,[2,9,11,12,35] and the calculated results reasonably reveal the experimental phenomenon. Therefore, the GGA functional is used to study the surface $O_2$ reaction on $TiO_2$ surfaces in our present and previous studies.[13,17]

The transition state (TS) search for the $O_2$ dissociation and diffusion processes was performed with the climb image nudged elastic band (CI-NEB) method.[36–38] The cutoff of the plane-wave kinetic energy is 400 eV, and the Monkhorst–Pack *k*-point mesh is $2 \times 2 \times 1$. The convergence criteria for the electronic and ionic relaxation are $10^{-4}$ eV and 0.05 eV $Å^{-1}$, respectively. Bader charge analysis is used to analyze the electronic transfer and distribution,[39] and in order to better describe the electron distribution of the transition state, the charge difference $\Delta N_{e^-}$ is calculated and defined as $\Delta N_{e^-} = N_{TS} - N_{initial}$. Here, $N_{TS}$ is the electron charges on adsorbed $O_2$ at the TS and $N_{initial}$ is the electron charges on adsorption $O_2$ at the initial configuration.

The lattice parameters for stoichiometric anatase are $a$ = 3.830 Å and $c$ = 9.613 Å with GGA, and they are $a$ = 3.907 Å and $c$ = 9.757 Å with GGA+U, which, respectively, correspond to the most stable structure by fitting the lattice parameter. In these calculations, a $3 \times 2$ surface supercell with 108 atoms is used to study $O_2$ adsorption and dissociation. In the supercell, there are three stoichiometric ($TiO_2$) structure layers, in which the

 

bottom stoichiometric $TiO_2$ layer is fixed to simulate the bulk structure, and the same supercell is used to study $O_2$ adsorption in other research groups.[9,11] The thickness of the vacuum layer on the top of each supercell is 10 Å, which is similar to our previous calculation.[13]

The adsorption energy of an $O_2$ molecule ($E_{O_2ad}$) or per dissociated O adatom ($E_{Oad}$) on an A-$TiO_2$ (101) surface is defined as:

$$E_{O_2ad} = E_{surf+O_2} - E_{surf} - E_{O_2} \quad (1)$$

$$E_{Oad} = E_{surf+O} - E_{surf} - \frac{1}{2}E_{O_2} \quad (2)$$

Here, $E_{surf+O_2}$ is the system energy of adsorbed $O_2$ molecules on an A-$TiO_2$ (101) slab; $E_{surf+O}$ is the system energy of one dissociated O adatom on an A-$TiO_2$ (101) slab; $E_{surf}$ is the system energy without the adsorbed $O_2$ molecule or O adatoms and $E_{O_2}$ is the energy of an $O_2$ molecule in the gas phase.

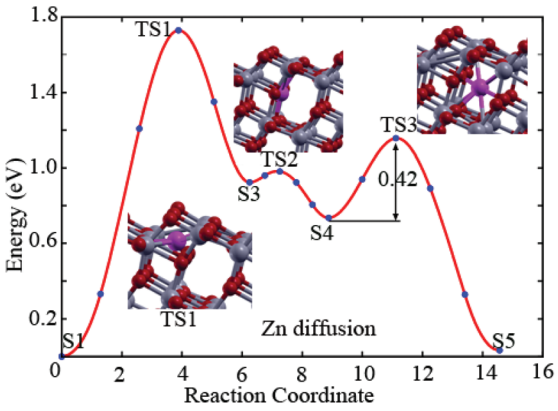


Fig. 2 Potential-energy profile for the diffusion of a Zn interstitial on the A-$TiO_2$ (101) surface and the energy is zero based on the initial structure S1.

## 3. Results and discussion

### 3.1 Defects

If a Zn interstitial is deposited on an A-$TiO_2$ (101) surface, there are several possible binding sites for the Zn atom on and near the A-$TiO_2$ (101) surface and the formation energies for these sites are calculated and listed in Table S1 (see the ESI†). From the results, two relatively stable surface and subsurface sites are identified, donated as S1 and S5 (see Fig. 1). For the S1 interstitial, the Zn atom is in the middle between two adjacent $O_{2c}$ atoms of the surface while for the S5 interstitial, the Zn atom is at the subsurface site and the formation energy of S5 (3.49 eV) is almost identical to that of S1 (3.47 eV). Meanwhile, in order to examine the stabilities of the S1 and S5 interstitials, the transformation from the interstitials S1 to S5 is calculated by the NEB method (see Fig. 2). During this transformation process, there are two metastable interstitials S3 and S4 (see Fig. S1 in the ESI†). S1 first diffuses to S3 and the energy barrier is 1.73 eV; subsequently, S3 instantaneously transforms to S4 with a barrier of only 0.06 eV. Finally, for S4 → S5, the barrier is 0.43 eV. Thus, in this path, the overall highest barrier is 1.73 eV from interstitials S1 to S5. In contrast, for the reverse diffusion from the interstitials S5 to S1 S5 → S4 → S3 → S1, the highest barrier is 1.12 eV (step S5 → S4) lower than that of path S1 to S5. The calculated results show that although a Zn interstitial relatively easily transforms from the subsurface to surface, the energy barrier for this process is still very high >1.10 eV. Therefore these two diffusion processes are difficult to occur and a Zn interstitial could stably stay on the surface S1 or at the subsurface S5 sites.

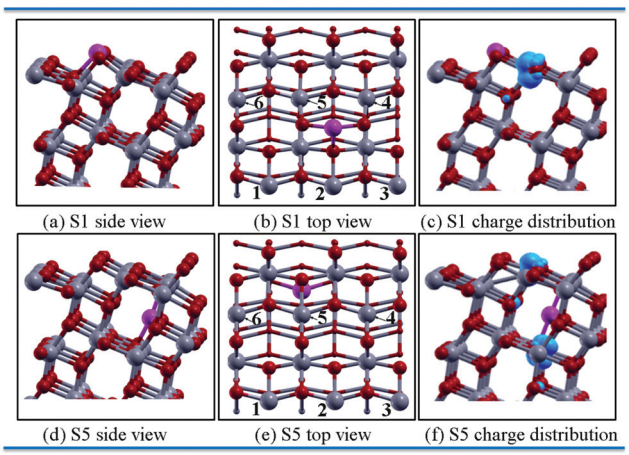


Fig. 1 S1 and S5 Zn interstitial configurations. The six $Ti_{5c}$ atoms on the surface are numbered from 1 to 6 which are the adsorption sites for the adsorbed oxygen molecule or adatoms. c and f show the distribution of two excess electrons induced by a Zn interstitial.

Furthermore, to describe the trapping states of electrons in $TiO_2$, we employ the GGA+U to calculate the excess charge distribution induced by a Zn interstitial and each defect gives rise to two excess electrons. Fig. 1(c) and (f) show that two excess electrons induced by the Zn interstitial transfer to the A-$TiO_2$ surface and are mainly localized on 3d orbits of lattice Ti atoms. For the S1 interstitial, most of the two excess electrons in 3d orbits distribute on surface Ti lattices (sites 5 and 6) while for the S5 interstitial, half of two excess electrons in 3d orbits are on a subsurface $Ti_{6c}$ atom. This charge localization suggests a stronger influence of the S1 interstitial (see Fig. 1) on the surface adsorption reactivity compared to that of the S5 interstitial.

### 3.2. One adsorbed $O_2$ molecule on a Zn-modified A-$TiO_2$(101) surface

The adsorption energies for an $O_2$ molecule at the various inequivalent $Ti_{5c}$ sites of S1 and S5 are calculated and the results (see Table 1) show that a Zn interstitial makes the adsorption process possible since an $O_2$ molecule is difficult to adsorb onto a clean A-$TiO_2$ (101) surface.[9,19] For the S1 surface, the adsorbed $O_2$ molecule releases most thermal energy at site 2 and the adsorption energy is −2.19 eV (see structure A1 Fig. 3). In the structure A1, the $O_2$ molecule has an O–O bond length of 1.46 Å close to the typical value for a

**Table 1** The adsorption energy $\Delta E$ (eV) of an oxygen molecule on a A-$TiO_2$ (101) surface

| S1 | $\Delta E$ | S5 | $\Delta E$ | $S1_H$ | $\Delta E$ | $S5_H$ | $\Delta E$ |
|---|---|---|---|---|---|---|---|
| 1 | −1.26 | 1 | −1.19 | 1 | −1.92 | 1 | −1.53 |
| 2 (A1) | −2.19 | 2 | −1.19 | 2 | −1.92 | 2 | −1.79 |
| 3 | −1.26 | 3 | −1.00 | 3 | −1.32 | 3 | −1.41 |
| 4 | −1.63 | 4 | −1.06 | 4 | −1.52 | 4 | −1.65 |
| 5 | −1.63 | 5 (B1) | −1.78 | 5 (C1) | −2.69 | 5 (D1) | −2.31 |
| 6 | −1.13 | 6 | −1.06 | 6 | −1.52 | 6 | −1.36 |

peroxide (1.49 Å) which means that partial excess electrons ($1.19e^-$ Bader charge analysis) from the A-$TiO_2$ (101) surface transfer to the $O_2$ $\pi^*$ orbitals and a peroxide radical is formed. The Ti–$O_{(1)}$ $O_{(2)}$ bond lengths are 2.05 and 1.90 Å, respectively, and the bond length between the Zn and $O_{(1)}$ atoms is 1.98 Å. For the S5 surface, the most favorable adsorption is at site 5 and configuration B1 is obtained. In structure B1, two new formed Ti–O bonds are both 1.86 Å long and the O–O bond length of the $O_2$ molecule is 1.44 Å, slightly shorter than that of A1. Meanwhile, the Bader analysis shows that electrons transferred to the adsorbed $O_2$ molecule for structure B1 are $0.13e^-$ less than those of A1 which is consistent with the fact that more excess electrons could transfer to the adsorption molecule on the S1 surface. Accordingly, the released thermal energy would be reduced during the adsorption process and the $O_2$ adsorption energy is −1.78 eV.

### 3.3. Reaction channels for an adsorbed $O_2$ molecule on a Zn-modified A-$TiO_2$ (101) surface

In this section, the calculations of $O_2$ dissociation were performed on and near the surface containing a Zn interstitial. As for these two adsorption configurations (A1 and B1), we first consider the dissociation process of adsorbed $O_2$ in structure A1. The schematic of this process is shown in path $Zn_{surf}$@$TiO_2$ (see Fig. 4) and the energy barrier is 1.50 eV. At the transition state TS4, the distance between $O_{(1)}$ and $O_{(2)}$ atoms is 1.87 Å which is much longer than the O–O bond length of the initial configuration A1. It suggests that the O–O bond has been broken. Bader charge analysis shows that the number of electrons transferred to $O_{(1)}$ and $O_{(2)}$ atoms are $0.46e^-$ and $0.96e^-$, respectively. After the TS4 structure A1 transforms into A2. In structure A2, $O_{(1)}$ and surface $O_{2c}$ form

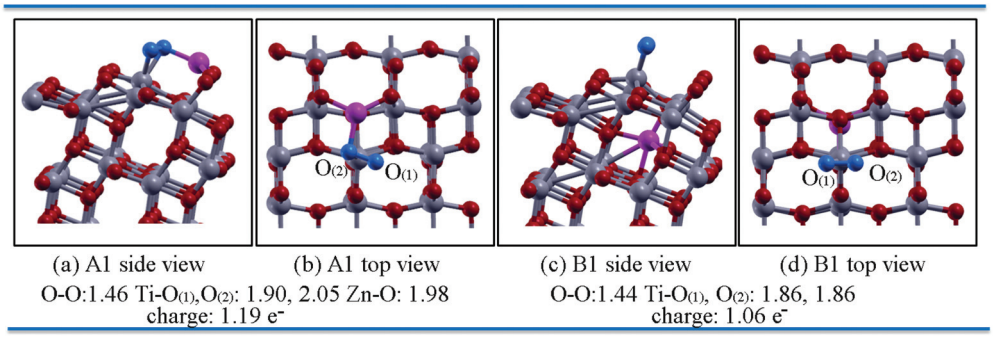


**Fig. 3** The most stable configurations of an $O_2$ molecule on a Zn-modified A-$TiO_2$ (101) surface (S1 and S5). $O_{(1)}$ and $O_{(2)}$ atoms are two adsorbed O atoms of the $O_2$ molecule. The number of electrons transferred to the adsorbed $O_2$ is calculated by the Bader charge analysis. The unit of the bond length is Å.

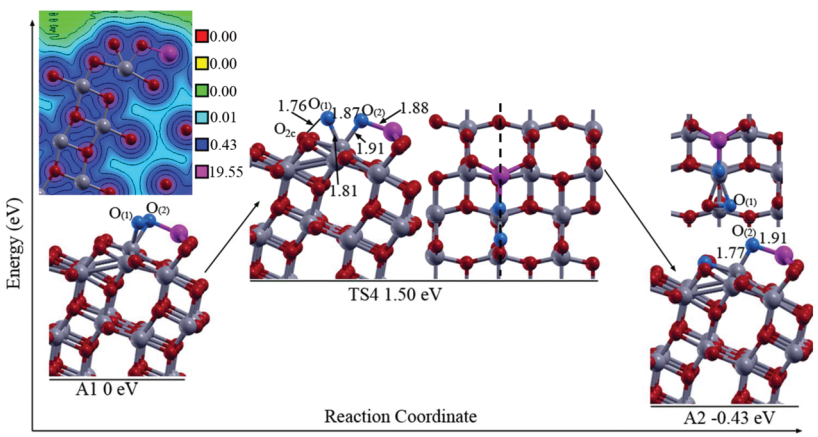


**Fig. 4** Calculated reaction path of $O_2$ dissociation from the structure A1 to A2 in path $Zn_{surf}$@$TiO_2$. There is a Zn interstitial on the surface and the adsorption configuration A1 is taken as the initial reference point.

new chemical bonds and both of them occupy the lattice $O_{2c}$ site. In this $Zn_{surf}@TiO_2$ path, the reaction energy for this exothermic process is 0.43 eV and the system significantly becomes more stable.

In the following, schematics of the dissociation of an $O_2$ molecule on the S5 surface are calculated and shown in Fig. 5 and two possible dissociation paths ($Zn_{sub1}@TiO_2$ and $Zn_{sub2}@TiO_2$) are searched since there are two final configurations (B2 and B3). For the first reaction path from structures B1 to B2 ($Zn_{sub1}@TiO_2$), the energy barrier is 1.32 eV, which is slightly lower than the barrier of the path in Fig. 4. At the transition state TS5, $O_{(1)}$ transforms onto a neighboring $Ti_{6c}$ and $O_{(2)}$ is still on the $Ti_{5c}$ atom. The Bader analysis shows that $O_{(1)}$ and $O_{(2)}$ obtain $1.39e^-$ and the charge difference $\Delta Ne^-$ is $0.33e^-$. The distance of the two O adatoms is 1.97 Å and the charge distribution is low between them, which means the O–O bond has been broken. The distance between $O_{(1)}$ and $O_{2c}$ is 1.71 Å and weak interaction may be produced between $O_{(1)}$ and $O_{2c}$ atoms since a few electrons transfer into the space between them (see Fig. 5(a)). Accordingly, the dissociation barrier slightly reduces by 0.18 eV compared with that of TS4. However, the reaction is endothermic and the system energy increases by 0.42 eV after dissociation. Thus this dissociation process is not energetically preferable to happen and two dissociated $O_{ad}$ atoms may again recombine to an $O_2$ molecule.

Suppose that structure B3 is in final configuration; the dissociation barrier is 1.13 eV from B1 to B3 which is lower than the barrier of the above two paths (TS4 and TS5). This process is also an endothermic reaction and the reaction energy is 0.26 eV. In the transition state TS6, the two adsorbed O atoms have been broken and the distance is 2.37 Å. Yet the $O_{(1)}$ atom again forms a new chemical bond with a surface $O_{2c}$ atom and the bond length is 1.42 Å. Meanwhile, the charge distribution between $O_{(1)}$ and $O_{2c}$ is high which suggests that the $O_{(1)}$ atoms are strongly bonded with the surface during TS6. Bader analysis shows that $O_{(1)}$ and $O_{(2)}$ obtain 0.5 and 1.06 $e^-$, respectively, and the charge difference $\Delta Ne^-$ is $0.17e^-$ higher than that of the path $Zn_{sub1}@TiO_2$. Therefore, if the adsorbed O atoms are bounded with the surface at the TS, more electron charges transfer to the O adatoms and thus the dissociation barrier would be reduced.

For the above three dissociation paths it can be seen that no matter if a Zn interstitial is on the surface or at the subsurface sites, all the $O_2$ molecules could be stably adsorbed onto the A-$TiO_2$ (101) surface and the Zn interstitial also contributes to $O_2$ dissociation especially a subsurface Zn interstitial; however, the dissociation barriers are still too high, >1.1 eV, and the $O_2$ dissociation is difficult to occur at room temperature. So if the $O_2$ dissociation barrier can be reduced, it will be more efficient to generate the O adatoms to oxidize adsorbed toxic gases on the A-$TiO_2$ surface. Based on our previous calculation,[25] surface H atoms could change the $O_2$ adsorption and dissociation on an A-$TiO_2$ surface. Therefore, it is interesting to study the synergistic effect of the Zn and H interstitials on $O_2$ adsorption and dissociation on an A-$TiO_2$ surface.

### 3.4. Effect of H on $O_2$ adsorption on a Zn-modified A-$TiO_2$ (101) surface

On a clean A-$TiO_2$ (101) surface, a H atom is preferable to adsorb onto the surface $O_{2c}$ atom.[40] For S1 and S5 surfaces, since a Zn interstitial is introduced into the clean $TiO_2$ surface, the different H adsorption sites around the Zn interstitial are considered and the adsorption energies are listed in Table S2 (see the ESI†). The calculated results show that the most stable sites of H atoms on the S1 and S5 surfaces are at sites 1 and 5, respectively, which are $S1_H$ and $S5_H$ configurations (see Fig. 6).

For an $O_2$ molecule on the $S1_H$ and $S5_H$ surfaces, there are six $Ti_{5c}$ adsorption sites on each surface and the calculated $O_2$ adsorption energies at different $Ti_{5c}$ sites are listed in Table 1. Compared with an $O_2$ molecule adsorbed on the S1 or S5 surface, it can be seen that the H atom further enhances $O_2$ adsorption at different sites of the $S1_H$ or $S5_H$ surface and more thermal energy is released during the adsorption process. On the $S1_H$ surface, C1 is the most stable adsorption configuration and the adsorption energy is −2.69 eV. For another most stable adsorption structure D1, the adsorption configuration and bond lengths are similar to those of B1 but

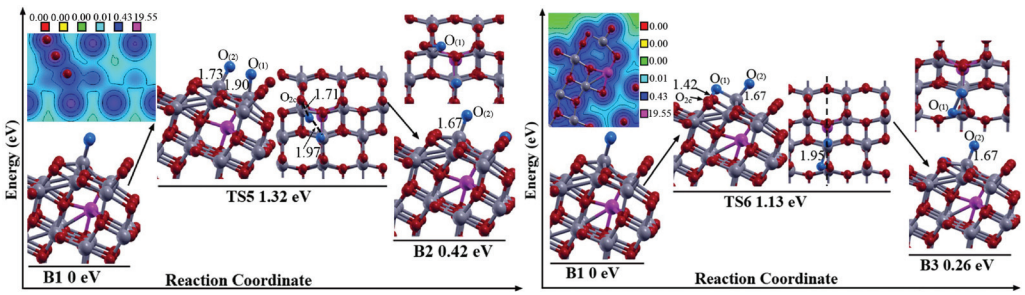


(a) $O_2$ dissociation in path $Zn_{sub1}@TiO_2$ (b) $O_2$ dissociation in path $Zn_{sub2}@TiO_2$

**Fig. 5** The two dissociation processes of an adsorbed $O_2$ molecule on the S5 surface are calculated by the NEB method. The structure B1 is the initial configuration and there are two final configurations B2 and B3. (a) $O_2$ dissociation in path $Zn_{sub1}@TiO_2$ and (b) $O_2$ dissociation in path $Zn_{sub2}@TiO_2$.

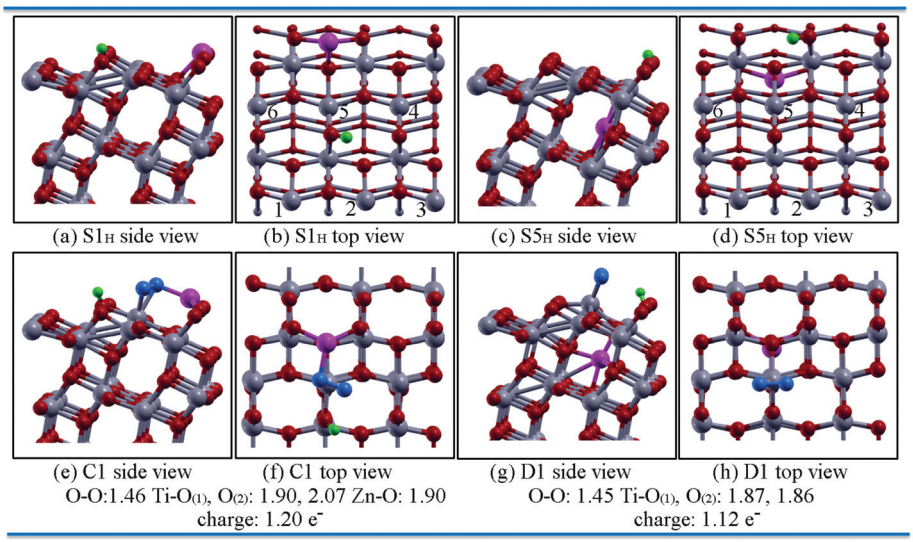


Fig. 6 The most stable configurations of a H atom adsorbed onto theS1 and S5 surfaces are structures $S1_H$ and $S5_H$, respectively, and accordingly, $O_2$ adsorbed onto $S1_H$ and $S5_H$ are configurations C1 and D1. Blue balls are two adsorbed O atoms.

the number of electrons transferred to the adsorbed $O_2$ molecule is $0.06e^-$ higher than that of B1; accordingly, the value of the adsorption energy for the $O_2$ molecule (−2.31 eV) is lowered compared with that of B1 (−1.78 eV). Since the initial adsorption configurations C1 and D1 are achieved (see Fig. 6), how an adsorbed $O_2$ molecule dissociates on the $S1_H$ and $S5_H$ surface is calculated and discussed in the next part.

### 3.5. Synergistic effect of the Zn and H interstitials on $O_2$ dissociation on an A-$TiO_2$ (101) surface

**3.5.1. $O_2$ dissociation in path $Zn_{surf}$@H-$TiO_2$.** For the initial structure C1, the adsorbed $O_2$ molecule dissociates and the reaction schematic is shown in Fig. 7. When an $O_2$ molecule is adsorbed at site 5 of the $S1_H$ surface (structure C1), the H adatom on $O_{2c}$ could diffuse to the $O_{(1)}$ adatom and the Ti–$O_{(1)}$ bond is broken forming an OOH radical. The barrier is 0.47 eV and the system becomes more stable after H diffusion. In the subsequent step C2 → TS8 → C3 (the barrier: 0.38 eV), the $O_{(1)}$ atom rotates a little and forms a new bond with the Zn interstitial while the Zn–$O_{(2)}$ bond is broken during the transition state TS8. After this transformation, the system energy slightly increases by 0.33 eV compared with that of C2. For the last reaction step, C3 → C4, C3 is the initial configuration and the $O_2$ molecule dissociates. The dissociation barrier is 0.52 eV which is much lower than those of the above three paths (TS4, TS5 and TS6, see Fig. 4 and 5). In this step, the configurations of two O adatoms of TS9 are similar to those of TS4, that is the O–O bond has been broken and no chemical bond forms between $O_{(1)}$ and $O_{2c}$ atoms which can be seen from the charge distribution of TS9. Yet the differences are that in TS9, the calculated $\Delta Ne^-$ is $0.67e^-$ which is $0.44e^-$ higher than that of TS4; meanwhile, the H atom stabilizes the $O_{(1)}$ adatom and

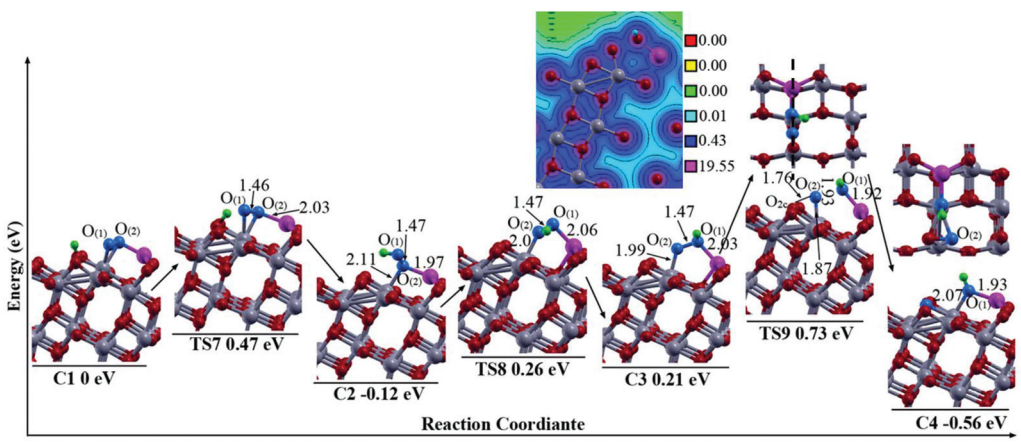


Fig. 7 Calculation of the reaction process of $O_2$ dissociation on the $S1_H$ surface (Path $Zn_{surf}$@H-$TiO_2$). C1 is the initial configuration and the highest energy barrier is 0.56 eV for this reaction process. The side view of the charge density of TS9 along the dashed line is shown in the figure.

 

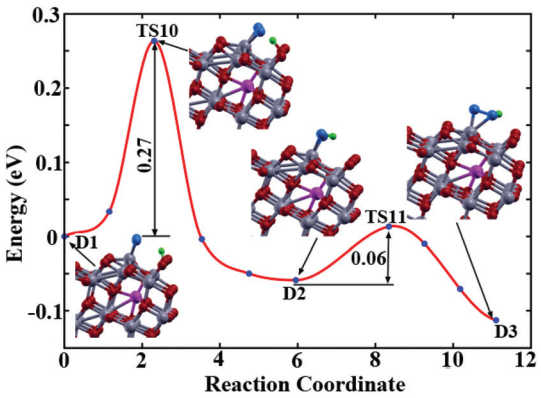


Fig. 8 The H diffusion in the configuration D1. The system energy of D1 is set to zero. After the diffusion, the H atom transforms from the surface $O_{2c}$ to the adsorbed $O_2$ molecule forming an OOH radical on the $S_{5H}$ surface.

thus it makes the dissociation barrier lower compared with that of TS4. For the whole reaction process C1 → C4, the total reaction energy for this exothermic process is 0.56 eV and the highest energy barrier is 0.52 eV which corresponds to the transformation from C3 to C4. This calculated result shows that although the adsorbed H atom makes the dissociation step more complex, it significantly lowers the $O_2$ dissociation barrier which would contribute to producing more active O adatoms on the surface and improving the oxidation activity of the A-$TiO_2$ surface.

**3.5.2. $O_2$ dissociation in path $Zn_{sub}$@H-$TiO_2$.** After an $O_2$ molecule is adsorbed at site 5 of the $S5_H$ surface, a stable adsorption configuration D1 is obtained. In D1, the surface H atom is attracted by the adsorbed $O_2$ molecule and the energy barrier for this transformation from D1 to D2 is 0.27 eV (see Fig. 8). As a result, an OOH radical is formed on the surface and the system energy is slightly reduced by 0.05 eV. Subsequently, the OOH radical in D2 can rotate counterclockwise by 90° and the system continues to release thermal energy. From structures D1 to D3, the total system energy reduces by 0.11 eV and the $O_2$ molecule becomes more stably adsorbed (see Fig. 8).

In the following, D3 is the initial configuration and the dissociation process of the $O_2$ molecule is calculated as shown in Fig. 9. Initially, the adsorbed OOH radical happens to dissociate and the energy barrier for this dissociation is 0.47 eV. In TS12, the distance between two O adatoms is 1.78 Å and there is less charge density between $O_{(1)}$ and $O_{(2)}$ atoms. This suggests that the O–O bond of the $O_2$ molecule is broken. For this dissociation step, since subsurface $O_{3c}$ atoms form stable Zn–O bonds with the subsurface Zn interstitial, the subsurface $O_{3c}$ atoms are passivated and their interaction with the surface $Ti_{5c}$ is weakened. As a result, the surface $Ti_{5c}$ can easily move outward to bind with two O adatoms during TS9 and the Bader charge analysis shows that $O_{(1)}$ and $O_{(2)}$ adatoms, respectively, obtain 0.68 and 1.19$e^-$ electron charges and the charge difference $\Delta Ne^-$ is 0.76$e^-$. Accordingly, the dissociation barrier is further reduced compared with that of TS6 in Fig. 5. After dissociation, a dangling O atom and an OH radical are produced on the $Ti_{5c}$ atom (see D4). Yet D4 is a metastable configuration and there will be an energetic driving force for the $O_{2c}$ atom to diffuse to a more stable site. *Via* the diffusion structure, D4 transforms to D5 and the protuberant $Ti_{5c}$ atom in structure D4 moves back to the original position. The energy barrier for this diffusion is 0.45 eV and this process is easy to happen. For the whole reaction path (Fig. 8 and 9) D1 → D2 → D3 → D4 → D5, the highest energy barrier is 0.47 eV, much lower than those of TS5 and TS6 (TS5 and TS6: 1.32 and 1.13 eV, respectively, see Fig. 5) and the system energy drops by 0.37 eV. It shows that with the help of a surface H atom, the process of $O_2$ dissociation becomes much easier on a subsurface Zn interstitial modified A-$TiO_2$ (101) surface and the system also becomes more stable after the dissociation reaction.

### 3.6. The analysis of ORR activity

On a Zn-modified A-$TiO_2$ (101) surface, regardless of whether the Zn atom is on the surface or at the subsurface site two

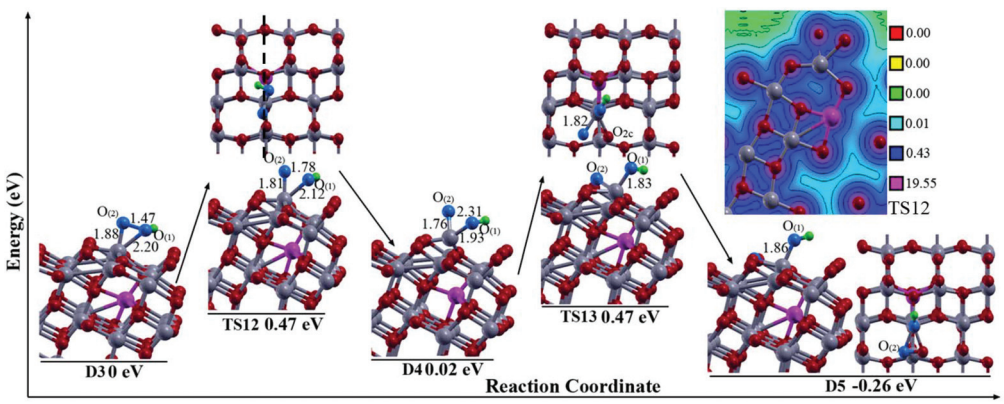


Fig. 9 Calculation of the reaction process of $O_2$ dissociation on the $S5_H$ surface (path $Zn_{sub}$@H-$TiO_2$). D3 is the initial configuration and the highest energy barrier is 0.47 eV for this reaction process. The side view of the charge density of TS12 along the dashed line is shown in the figure.

Table 2 The highest reaction barrier ($\Delta E_a$) for the dissociation of an $O_2$ molecule on an A-$TiO_2$ (101) surface. In order to examine the possibility of the reaction process, the attempt frequency $\nu$ for the $O_2$ dissociation at the room temperature of 300 K is calculated by the equation: $\nu_0 \sim \nu_0 e^{-(\Delta E_a/KT)}$ using the typical value $\nu_0 \sim 10^{13}$ $s^{-1}$ for the attempt frequency

| Initial | Final | $\Delta E_a$ (eV) | $\nu$ |
|---|---|---|---|
| A1 | A2 | 1.50 | 0 |
| B1 | B2 | 1.32 | 0 |
| B1 | B3 | 1.13 | 0 |
| C1 | C4 | 0.52 | $10^4$ |
| D1 | D5 | 0.47 | $10^5$ |

unpaired electrons induced by the Zn atom mainly transfer to Ti lattices. If an $O_2$ molecule is approached and adsorbed onto the A-$TiO_2$ (101) surface, partial excess charges would transfer to the adsorbed $O_2$ molecule from the surface. For the $O_2$ reaction process on a Zn-modified A-$TiO_2$ surface, although the Zn interstitial makes $O_2$ adsorption and dissociation possible, the energy barriers are so high (>1.10 eV, see Table 2) that the $O_2$ molecule is difficult to dissociate to produce the O adatoms. Our further research studies show that if a H atom is introduced on the Zn-modified A-$TiO_2$ (101) surface, it could significantly enhance $O_2$ adsorption and greatly reduce the energy barriers of $O_2$ dissociation. The highest dissociation barriers for two paths are, respectively, 0.52 and 0.47 eV lower than the $O_2$ dissociation barrier on a Pt (111) surface (0.86 eV).[41] A simple estimate is that these two processes are rather frequent (0.52 eV: $10^4$ $s^{-1}$ 0.47 eV: $10^5$ $s^{-1}$) at the temperature of 300 K. Meanwhile, in order to better understand mechanisms of $O_2$ dissociation, we further analyzed the calculated dissociation processes and found that the dissociation barriers decrease almost linearly with the increase of the $\Delta Ne^-$ as shown in Fig. 10, which are not directly related with the strength of $O_2$ adsorption. This suggests that the charge difference $\Delta Ne^-$ is one of the important parameters determining the activity of the supported Zn single atom toward $O_2$ dissociation on the A-$TiO_2$ (101) surface.

In fact a good ORR catalytic activity requires intermediate oxygen bonding to the active site facilitating both O–O bond breaking and subsequent oxidation reactions of O atoms. If an adsorbed $O_2$ molecule is easy to dissociate on the surface of a catalyst and the dissociated oxygen atoms can be relatively easily desorbed from the surface, this catalyst has good activity for oxidizing adsorbed toxic gases. To examine the ability of dissociated O atoms for the subsequent oxidation reaction, we calculate the adsorption energies of two O adatoms in paths $Zn_{surf}$@H-$TiO_2$ and $Zn_{sub}$@H-$TiO_2$. For C4 in Fig. 7, the O atom in the OH radical forms a bond with the Zn interstitial and the calculated adsorption energy of this O adatom is −3.12 eV, which means that OH is strongly bonded with the $TiO_2$ surface and difficult to release from the surface, losing the oxidation activity. The adsorption energy of the other adatom, $O_{(2)}$, is 0.30 eV, similar to that of previous results[17] and thus this O adatom could be easy to desorb from the surface. For the final structure D5 in Fig. 9, the adsorption energy of the O atom in the OH radical is −1.53 eV, which can nearly match that on the Pt (111) surface (−1.26 eV)[42,43] and the $O_{(2)}$ adsorption energy is 0.25 eV. That is, two dissociated O atoms could desorb relatively easily from the $S5_H$ surfaces for the subsequent oxidation reaction. Therefore, our DFT results show that the surface H atom and the subsurface Zn interstitial could facilitate both O–O bond breaking and the subsequent oxidation reaction of O atoms.

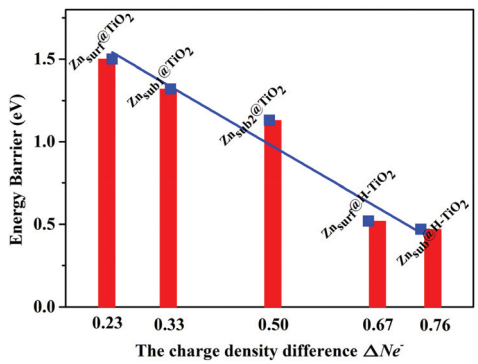


Fig. 10 The relationship between $O_2$ dissociation barrier and the charge density difference $\Delta Ne^-$.

## Conclusions

The first-principles calculation coupled with the nudged elastic band method is used to investigate how zinc and hydrogen interstitials affect the energetics and mechanisms of the $O_2$ reduction reaction (ORR) on an A-$TiO_2$ (101) surface. In this work, we found that when a Zn atom is introduced on and near the surface and subsurface Zn interstitials, all could contribute to $O_2$ adsorption and dissociation; yet the dissociation barriers are too high. Further study shows that the surface H adatom could significantly change $O_2$ adsorption and dissociation on the Zn-modified surface. Specially with the synergistic effect of subsurface Zn and surface H interstitials, the adsorbed $O_2$ is easy to dissociate and the highest reaction barrier is only 0.47 eV suggesting that the reaction process could frequently happen even at the room temperature of 300 K; meanwhile, the dissociated O adatoms are also easy to desorb from the surface for the subsequent oxidation reaction. Consequently, our theoretical study shows that after the subsurface Zn modified anatase $TiO_2$ particles are hydrogenated, they would become efficient catalysts for $O_2$ adsorption and dissociation, which provides a theoretical support to design high ORR activity catalysts of $TiO_2$.

## Conflicts of interest

There are no conflicts to declare.

## Acknowledgements

This work is supported by the National Natural Science Foundation of China (No. 11275142, 11575129, and 11605232), the Natural Science Foundation of Anhui Province of China (No. 1708085QE101) and the Key Program of the Higher Education Institutions of Henan Province (No. 16A140003).

## References

1 M. A. Henderson, A surface science perspective on photocatalysis, *Surf. Sci. Rep.*, 2011, **66**, 185–297.
2 Y.-F. Li, Z.-P. Liu, L. Liu and W. Gao, Mechanism and activity of photocatalytic oxygen evolution on titania anatase in aqueous surroundings, *J. Am. Chem. Soc.*, 2010, **132**, 13007–13015.
3 F. Huang, Q. Li, G. J. Thorogood, Yi.-B. Cheng and R. A. Caruso, Zn-doped $TiO_2$ electrodes in dye-sensitized solar cells for enhanced photocurrent, *J. Mater. Chem.*, 2012, **22**, 17128–17132.
4 S. In, A. Orlov, R. Berg, F. García, S. Pedrosa-Jimenez, M. S. Tikhov, D. SWright and R. M. Lambert, Effective visible light-activated B-doped and B N-codoped $TiO_2$ photocatalysts, *J. Am. Chem. Soc.*, 2007, **129**, 13790–13791.
5 S. Khan, H. Cho, D. Kim, S. S. Han, K. H. Lee, S.-H. Cho, T. Song and H. Choi, Defect engineering toward strong photo-catalysis of Nb-doped anatase $TiO_2$: Computational predictions and experimental verications, *Appl. Catal. B*, 2017, **206**, 520–530.
6 H. Gerischer and A. Heller, The role of oxygen in photooxidation of organic molecules on semiconductor particles, *J. Phys. Chem.*, 1991, **95**, 5261–5267.
7 C. Song and J. Zhang, Electrocatalytic oxygen reduction reaction, in *PEM fuel cell electrocatalysts and catalyst layers*, Springer, 2008, pp. 89–134.
8 V. Stamenkovic, B. Simon Mun, K. J. J. Mayrhofer, P. N. Ross, N. M. Markovic, J. Rossmeisl, J. Greeley and J. K. Nrskov, Changing the activity of electrocatalysts for oxygen reduction by tuning the surface electronic structure, *Angew. Chem. Int. Ed.*, 2006, **45**, 2897–2901.
9 U. Aschauer, J. Chen and A. Selloni, Peroxide and superoxide states of adsorbed $O_2$ on anatase $TiO_2$ (101) with subsurface defects, *Phys. Chem. Chem. Phys.*, 2010, **12**, 12956–12960.
10 C. L. Muhich, Y. Zhou, A. M. Holder, A. W. Weimer and C. B. Musgrave, Effect of surface deposited Pt on the photoactivity of $TiO_2$, *J. Phys. Chem. C*, 2012, **116**, 10138–10149.
11 M. Setvin, U. Aschauer, P. Scheiber, Y.-F. Li, W. Hou, M. Schmid, A. Selloni and U. Diebold, Reaction of $O_2$ with subsurface oxygen vacancies on $TiO_2$ anatase (101), *Science*, 2013, **341**, 988–991.
12 Y.-F. Li, U. Aschauer, J. Chen and A. Selloni, Adsorption and reactions of $O_2$ on anatase $TiO_2$, *Acc. Chem. Res.*, 2014, **47**, 3361–3368.
13 L. Liu, Q. Liu, Y. Zheng, Z. Wang, C. Pan and W. Xiao, $O_2$ adsorption and dissociation on a hydrogenated anatase (101) surface, *J. Phys. Chem. C*, 2014, **118**, 3471–3482.
14 J. G. Wang and B. Hammer, Role of Au+in supporting and activating $Au_7$ on $TiO_2$ (110), *Phys. Rev. Lett.*, 2006, **97**, 136107.
15 H. Cheng and A. Selloni, Energetics and diffusion of intrinsic surface and subsurface defects on anatase $TiO_2$(101), *J. Chem. Phys.*, 2009, **131**, 054703.
16 H. Cheng and A. Selloni, Surface and subsurface oxygen vacancies in anatase $TiO_2$ and differences with rutile, *Phys. Rev. B: Condens. Matter Mater. Phys.*, 2009, **79**, 092101.
17 L. Liu, Q. Liu, W. Xiao, C. Pan and Z. Wang, $O_2$ adsorption and dissociation on an anatase (101) surface with a subsurface Ti interstitia, *Phys. Chem. Chem. Phys.*, 2016, **18**, 4569–4576.
18 C. Lin, Y. Song, L. Cao and S. Chen, Oxygen reduction catalyzed by Au-$TiO_2$ nanocomposites in alkaline media, *ACS Appl. Mater. Interfaces*, 2013, **5**, 13305–13311.
19 C. L. Muhich, J. Y. Westcott IV, T. Fuerst, A. W. Weimer and C. B. Musgrave, Increasing the photocatalytic activity of anatase $TiO_2$ through B C and N doping, *J. Phys. Chem. C*, 2014, **118**, 27415–27427.
20 L. Chevallier, A. Bauer, S. Cavaliere, R. Hui, J. Rozire and D. J. Jones, Mesoporous nanostructured Nb-doped titanium dioxide microsphere catalyst supports for PEM fuel cell electrodes, *ACS Appl. Mater. Interfaces*, 2012, **4**, 1752–1759.
21 T. Arashi, J. Seo, K. Takanabe, J. Kubota and K. Domen, Nb-doped $TiO_2$ cathode catalysts for oxygen reduction reaction of polymer electrolyte fuel cells, *Catal. Today*, 2014, **233**, 181–186.
22 E. N. Alvar, B. Zhou and S. Holger Eichhorn, Carbon-embedded mesoporous Nb-doped $TiO_2$ nanofibers as catalyst support for the oxygen reduction reaction in pem fuel cells, *J. Mater. Chem. A*, 2016, **4**, 6540–6552.
23 X. Han and G. Shao, Theoretical prediction of p-type transparent conductivity in Zn-doped $TiO_2$, *Phys. Chem. Chem. Phys.*, 2013, **15**, 9581–9589.
24 Y. Wang, R. Zhang, J. Li, L. Li and S. Lin, First- principles study on transition metal-doped anatase $TiO_2$, *Nanoscale Res. Lett.*, 2014, **9**, 1–8.
25 L. Liu, Z. Wang, C. Pan, W. Xiao and K. Cho, Effect of hydrogen on $O_2$ adsorption and dissociation on a $TiO_2$ anatase (001) surface, *ChemPhysChem*, 2013, **14**, 996–1002.
26 G. Kresse and J. Hafner, Ab initio molecular dynamics for liquid metals, *Phys. Rev. B: Condens. Matter Mater. Phys.*, 1993, **47**, 558–561.
27 G. Kresse and J. Hafner, Ab Initio Molecular-Dynamics Simulation of the Liquid-Metal-Amorphous-Semi- conductor Transition in Germanium, *Phys. Rev. B: Condens. Matter Mater. Phys.*, 1994, **49**, 14251.
28 G. Kresse and J. Furthmuller, Efficiency of *ab initio* total energy calculations for metals and semiconductors using a plane-wave basis set, *Comput. Mater. Sci.*, 1996, **6**, 15–50.
29 P. E. Blöchl, Projector augmented-wave method, *Phys. Rev. B: Condens. Matter Mater. Phys.*, 1994, **50**, 17953.

30 G. Kresse and D. Joubert, From ultrasoft pseudopotentials to the projector augmented-wave method, *Phys. Rev. B: Condens. Matter Mater. Phys.*, 1999, **59**, 1758–1775.
31 G. Kresse and J. Hafner, Ab initiomolecular dynamics for open-shell transition metals, *Phys. Rev. B: Condens. Matter Mater. Phys.*, 1993, **48**, 13115–13118.
32 B. J. Morgan and G. W. Watson, GGA+U description of lithium intercalation into anatase $TiO_2$, *Phys. Rev. B: Condens. Matter Mater. Phys.*, 2010, **82**, 144119.
33 M. F. Camellone and D. Marx, On the impact of solvation on a $Au/TiO_2$ nanocatalyst in contact with water, *J. Phys. Chem. Lett.*, 2013, **4**, 514–518.
34 Y. Du, N. A. Deskins, Z. Zhang, Z. Dohnalek, M. Dupuis and I. Lyubinetsky, Formation of O adatom pairs and charge transfer upon $O_2$ dissociation on reduced $TiO_2$ (110), *Phys. Chem. Chem. Phys.*, 2010, **12**, 6337–6344.
35 S. Tan, Y. Ji, Y. Zhao, A. Zhao and B. Wang, Molecular oxygen adsorption behaviors on the rutile $TiO_2$(110)-1·1 surface: An in Situ study with low-temperature scanning tunneling microscopy, *J. Am. Chem. Soc.*, 2011, **133**, 2002–2009.
36 H. Jónsson, G. Mills and K. W. Jacobsen, Nudged elastic band method for nding minimum energy paths of transitions, in *Classical and Quantum Dynamics in Condensed Phase Simulations*, ed. B. J. Berne, G. Ciccotti and D. F. Coker, World Scientic, Singapore, 1998, pp. 385.
37 G. Henkelman, B. P. Uberuaga and H. Jonsson, A climbing image nudged elastic band method for finding saddle points and minimum energy paths, *J. Chem. Phys.*, 2000, **113**, 9901–9904.
38 G. Henkelman and H. Jonsson, Improved tangent estimate in the nudged elastic band method for finding minimum energy paths and saddle points, *J. Chem. Phys.*, 2000, **113**, 9978–9985.
39 E. Sanville, S. D. Kenny, R. Smith and G. Henkelman, Improved grid-based algorithm for bader charge allocation, *J. Comput. Chem.*, 2007, **28**, 899–908.
40 U. Aschauer and A. Selloni, Hydrogen interaction with the anatase $TiO_2$(101) surface, *Phys. Chem. Chem. Phys.*, 2012, **14**, 16595–16602.
41 A. Eichler and J. Hafner, Molecular precursors in the dissociative adsorption of $O_2$ on Pt (111), *Phys. Rev. Lett.*, 1997, **79**, 4481.
42 A. Hellman, S. Klacar and H. Grnbeck, Low temperature CO oxidation over supported ultrathin MgO films, *J. Am. Chem. Soc.*, 2009, **131**, 16636–16637.
43 Y. Zheng, W. Xiao, M. Cho and K. Cho, Density functional theory calculations for the oxygen dissociation on nitrogen and transition metal doped graphenes, *Chem. Phys. Lett.*, 2013, **586**, 104–107.